

## Liouvillian Dynamics of the Hopf Bifurcation

P. Gaspard<sup>1</sup> and S. Tasaki<sup>2</sup>

<sup>1</sup>*Center for Nonlinear Phenomena and Complex Systems,  
Faculté des Sciences, Université Libre de Bruxelles,  
Campus Plaine, Code Postal 231, B-1050 Brussels, Belgium*

<sup>2</sup>*Advanced Institute for Complex Systems,  
Department of Applied Physics,  
School of Science and Engineerings,  
Waseda University,  
3-4-1 Okubo, Shinjuku-ku,  
Tokyo 169-8555, Japan*

Two-dimensional vector fields undergoing a Hopf bifurcation are studied in a Liouville-equation approach. The Liouville equation rules the time evolution of statistical ensembles of trajectories issued from random initial conditions, but evolving under the deterministic dynamics. The time evolution of the probability densities of such statistical ensembles can be decomposed in terms of the spectrum of the resonances (i.e., the relaxation rates) of the Liouvillian operator or the related Frobenius-Perron operator. The spectral decomposition of the Liouvillian operator is explicitly constructed before, at, and after the Hopf bifurcation. Because of the emergence of time oscillations near the Hopf bifurcation, the resonance spectrum turns out to be complex and defined by both relaxation rates and oscillation frequencies. The resonance spectrum is discrete far from the bifurcation and becomes continuous at the bifurcation. This continuous spectrum is caused by the critical slowing down of the oscillations occurring at the Hopf bifurcation and it leads to power-law relaxation as  $1/\sqrt{t}$  of the probability densities and statistical averages at long times  $t \rightarrow \infty$ . Moreover, degeneracy in the resonance spectrum is shown to yield a Jordan-block structure in the spectral decomposition.

PACS numbers: 05.45.-a, 05.10.-a, 82.40.Bj

### I. INTRODUCTION

In many nonlinear dynamical systems, sensitivity to initial conditions as well as bifurcations deeply affect the time evolution. In these cases, trajectories issued from random initial conditions evolve differently, leading to a statistical distribution of the trajectories over the phase space. Such statistical time evolutions are of great experimental importance because many time-dependent phenomena are characterized by the time-correlation function between the statistical distribution of initial conditions and an observable quantity measured at some later time. In this context, a major preoccupation is to understand, thanks to these time-correlation functions, how the system relaxes at long times toward a certain stationary or time-dependent state.

Recently, new methods have been developed in order to predict the behavior of the time-correlation functions and, in particular, to calculate the relaxation rates of the system [1–4]. These methods are based on a probabilistic approach in which the statistical ensembles of trajectories are described in terms of probability densities defined in the phase space of the system [1]. The deterministic dynamics is known to induce the time evolution of the probability densities. Since the probability is locally conserved in phase space, the density obeys a conservation equation called the generalized Liouville equation [1]. Integrating the Liouville equation in time, we obtain the so-called Frobenius-Perron operator, which gives the probability density at current time in terms of the initial probability density of the randomly distributed initial data [4].

During the last decade, much work has been devoted to the Frobenius-Perron operator of different systems [2–10] and to the related Pollicott-Ruelle resonances [11, 12]. These resonances are defined as the generalized eigenvalues of the Frobenius-Perron operator or of the Liouvillian operator and they control the relaxation of the probability density toward the stationary state if it exists. Accordingly, their knowledge provides us with the time-asymptotic behavior of the time-correlation functions which characterize the system. In this context, we have previously obtained the spectrum of the Liouvillian operator for the pitchfork bifurcation [8]. In such a bifurcation, all the asymptotic states are stationary.

The purpose of the present paper is to study the Liouvillian dynamics of systems undergoing a Hopf bifurcation [13], which is known to generate oscillatory time behavior. The importance of the Hopf bifurcation holds in the fact that

this bifurcation provides a unique mechanism to explain the emergence of oscillatory behavior in far-from-equilibrium physico-chemical systems [1]. This bifurcation has been much studied at the level of the trajectories [1, 14–16]. The effect of stochastic (or noisy) perturbations on the Hopf bifurcation have also been studied in the frameworks of the Langevin, Fokker-Planck, and master equations [17–19], as well as in the numerical simulation of far-from-equilibrium chemical reactions [20, 21]. Our aim is here to develop the probabilistic study of the Hopf bifurcation at the level of the Liouville equation, in which the dynamics is considered to be deterministic, so that the effect of the stochastic fluctuations will *not* be considered in the present paper. Instead our study deals with the deterministic time evolution of statistical ensembles of trajectories issued from random initial conditions and the characterization of such evolution in terms of the spectrum of the Liouville equation.

Near a Hopf bifurcation, we expect the emergence of sustained oscillations so that the asymptotic states are no longer stationary in contrast with the asymptotic behavior near a pitchfork bifurcation. After the Hopf bifurcation, a periodic orbit – also called limit cycle – coexists with an unstable stationary point in phase space. A fundamental problem is therefore to understand how the emergence of oscillations manifests itself in the spectrum of the Liouville equation before, at, and after the Hopf bifurcation.

In systems with periodic orbits, the Liouvillian spectrum can in principle be calculated with the Cvitanović-Eckhardt trace formula [3] and its cycle expansion [2]. In this periodic-orbit theory of classical systems, the Liouvillian or Pollicott-Ruelle resonances can be obtained as the zeros of a Selberg-Smale zeta function [2–4]. However, in periodic-orbit theory, few results are known about systems undergoing bifurcations such as the Hopf bifurcation. In this regard, the coexistence of a stationary point with a periodic orbit is of very special interest because the stationary point contributes to the Liouvillian spectrum by extra resonances which are not predicted by the periodic-orbit theory. In the present paper, one of our goals is to show that the periodic-orbit theory can be extended to incorporate the effects of the coexisting stationary points.

Furthermore, we shall explicitly construct the eigenstates and other root states which are associated with the Liouvillian resonances. We shall see that special methods are required to carry out this construction in the presence of certain degeneracies between a resonance of the limit cycle and another one associated with the coexisting unstable stationary point. Indeed, such degeneracies can lead to Jordan-block structures involving Jordan-type root states beside the standard eigenstates. The knowledge of all these eigenstates and other root states provides us with the asymptotic time dependence of all the possible time-correlation functions of a system undergoing a Hopf bifurcation.

The plan of the paper is the following. The general theory of the Liouvillian dynamics is summarized in Sec. II where an extended trace formula including the effect of the stationary points is derived. In this way, we obtain explicit expressions for the Liouvillian resonances of generic systems with stationary points coexisting with a periodic attractor. In Sec. III, we present the Hopf bifurcation and we derive the Liouvillian spectrum for a general Hopf bifurcation from the extended trace formula. In Sec. IV, we derive the detailed spectral decomposition of the normal form near the Hopf bifurcation: before, at, and after criticality. Conclusions are drawn in Sec. V.

## II. GENERAL THEORY

### A. Time evolution of statistical ensembles

We consider a deterministic dynamical system given by a set of first-order differential equations of the form

$$\dot{\mathbf{X}} = \mathbf{F}(\mathbf{X}; \boldsymbol{\mu}), \quad (1)$$

where  $\mathbf{X}$  are variables belonging to a phase space  $\mathcal{M} \subseteq \mathbb{R}^d$ ,  $\mathbf{F}$  is a time-independent vector field defined in  $\mathcal{M}$ ,  $\boldsymbol{\mu}$  is a set of parameters, and the dot denotes a derivative with respect to the time  $t$ :  $\dot{\mathbf{X}} = d\mathbf{X}/dt$ . The vector field (1) induces a one-parameter time-continuous group called the *flow*, which maps each initial condition onto the position at a current time  $t$

$$\mathbf{X}_t = \Phi^t \mathbf{X}_0, \quad (2)$$

and which defines the trajectory  $\mathbf{X}_t$  issued from the initial condition  $\mathbf{X}_0$ .

If we know the flow (2), we can infer the properties of the time evolution of a statistical ensemble of trajectories  $\{\mathbf{X}_t^{(i)} = \Phi^t \mathbf{X}_0^{(i)}\}_{i=1}^{\infty}$  issued from random initial conditions  $\{\mathbf{X}_0^{(i)}\}_{i=1}^{\infty}$ . If the initial conditions are randomly distributed, we have to introduce the probability density of the initial conditions as

$$\rho_0(\mathbf{X}) = \lim_{N \rightarrow \infty} \frac{1}{N} \sum_{i=1}^N \delta(\mathbf{X} - \mathbf{X}_0^{(i)}), \quad \text{such that} \quad \int \rho_0(\mathbf{X}) d\mathbf{X} = 1, \quad (3)$$

which is assumed to be a smooth function in phase space. In an experiment where a statistical ensemble of trajectories of the dynamical system (1) evolves in time from random initial conditions, a quantity of great importance is the mean value, i.e., the statistical average of an observable quantity defined over the phase space by the function  $A(\mathbf{X})$ . At the current time  $t$ , the mean value of this observable is given by

$$\langle A \rangle_t = \lim_{N \rightarrow \infty} \frac{1}{N} \sum_{i=1}^N A(\Phi^t \mathbf{X}_0^{(i)}) = \int A(\Phi^t \mathbf{X}) \rho_0(\mathbf{X}) d\mathbf{X} = \int A(\mathbf{X}) \rho_t(\mathbf{X}) d\mathbf{X}, \quad (4)$$

where we have introduced the probability density at time  $t$  as

$$\rho_t(\mathbf{X}) = \int \delta(\mathbf{X} - \Phi^t \mathbf{Y}) \rho_0(\mathbf{Y}) d\mathbf{Y} = \left| \frac{\partial \Phi^{-t}}{\partial \mathbf{X}}(\mathbf{X}) \right| \rho_0(\Phi^{-t} \mathbf{X}) \equiv (\hat{P}^t \rho_0)(\mathbf{X}), \quad (5)$$

which defines the so-called Frobenius-Perron operator  $\hat{P}^t$ . We notice that a time-dependent mean value such as (4) defines a time-correlation function between the initial density  $\rho_0$  and the observable quantity  $A$  measured at time  $t$ . Therefore, the present framework describes the time evolution of general time-correlation functions.

Since the probability is conserved locally in phase space, the probability density obeys a partial differential equation of continuity known as the Liouville equation [1, 22]

$$\partial_t \rho_t = -\text{div}(\mathbf{F} \rho_t) \equiv \hat{L} \rho_t. \quad (6)$$

The Liouvillian operator  $\hat{L}$  is the generator of the Frobenius-Perron operator:  $\hat{P}^t = \exp(\hat{L}t)$ . The Frobenius-Perron operator provides therefore the global time evolution of the density over a finite time interval, while the Liouvillian operator rules the time evolution over an infinitesimal time evolution. In this regard, both operators and their properties are thus interconnected.

For conservative systems, the Liouvillian operator defined as in Eq. (6) is anti-Hermitian. However, for dissipative systems, the Liouvillian operator is not anti-Hermitian. This property has its origin in the non-preservation of phase-space volumes in a dissipative system for which

$$\hat{L} + \hat{L}^\dagger = -(\text{div } \mathbf{F}) \hat{I}, \quad (7)$$

where  $\hat{L}^\dagger = \mathbf{F} \cdot \partial_{\mathbf{X}}$  is the adjoint of  $\hat{L}$  and  $\hat{I}$  is the identity operator. Therefore, the spectral theory of the Liouvillian operator and of the related Frobenius-Perron operator is in general more complicated than for Hermitian or anti-Hermitian operators.

## B. Spectral decomposition

The time evolution of statistical ensembles can be characterized in terms of the relaxation rates toward the stationary invariant measure which is reached after long times. These relaxation rates can be considered as complex eigenvalues  $\{s_j\}$  of the Liouvillian operator with  $\text{Re } s_j \leq 0$ . Since the Liouvillian operator is not anti-Hermitian we should expect in general that the left and right eigenstates be different and that Jordan-block structures be possible [23]. In the case of a spectrum of eigenvalues, a possible spectral decomposition of the Liouvillian operator is thus

$$\hat{L} = \sum_j |\psi_j\rangle s_j \langle \tilde{\psi}_j| + \sum_k (|\psi_{k,1}\rangle \quad |\psi_{k,2}\rangle) \begin{pmatrix} s_k & 1 \\ 0 & s_k \end{pmatrix} \begin{pmatrix} \langle \tilde{\psi}_{k,1}| \\ \langle \tilde{\psi}_{k,2}| \end{pmatrix} + \dots, \quad (8)$$

with possible higher-dimensional Jordan blocks. The right and left root states  $\{|\psi_{k,l}\rangle, \langle \tilde{\psi}_{k,l}|\}$  are supposed to form a complete biorthonormal basis

$$\begin{aligned} \langle \tilde{\psi}_{l,m} | \psi_{l',m'} \rangle &= \delta_{ll'} \delta_{mm'}, \\ \sum_{l,m} |\psi_{l,m}\rangle \langle \tilde{\psi}_{l,m}| &= \hat{I}, \end{aligned} \quad (9)$$

with  $l = j, k, \dots$  and  $m = \emptyset, 1, 2, \dots$

As a consequence of Eq. (8), the Frobenius-Perron operator has the eigenvalues  $\{\exp(s_j t)\}$  and the spectral decomposition

$$\hat{P}^t = e^{\hat{L}t} = \sum_j |\psi_j\rangle e^{s_j t} \langle \tilde{\psi}_j| + \sum_k (|\psi_{k,1}\rangle \quad |\psi_{k,2}\rangle) e^{s_k t} \begin{pmatrix} 1 & t \\ 0 & 1 \end{pmatrix} \begin{pmatrix} \langle \tilde{\psi}_{k,1}| \\ \langle \tilde{\psi}_{k,2}| \end{pmatrix} + \dots. \quad (10)$$

Many works [4–6, 8, 11, 12] have shown that such eigenvalue problems have to be conceived on suitable functional spaces of smooth enough test functions in order to give a meaning to the right and left eigenstates and other root states which turn out to be Schwartz distributions [24], as well as to justify the spectral decomposition which holds on a suitable Gel'fand triplet [25].

According to Eq. (4), the spectral decomposition (10) provides the time evolution of the mean value of an observable in the following form

$$\begin{aligned} \langle A \rangle_t &= \langle A | \hat{P}^t | \rho_0 \rangle \\ &= \sum_j \langle A | \psi_j \rangle e^{s_j t} \langle \tilde{\psi}_j | \rho_0 \rangle \\ &+ \sum_k (\langle A | \psi_{k,1} \rangle \langle A | \psi_{k,2} \rangle) e^{s_k t} \begin{pmatrix} 1 & t \\ 0 & 1 \end{pmatrix} \begin{pmatrix} \langle \tilde{\psi}_{k,1} | \rho_0 \rangle \\ \langle \tilde{\psi}_{k,2} | \rho_0 \rangle \end{pmatrix} + \dots \end{aligned} \quad (11)$$

We observe that the right root states are distributions acting on the observables while the left root states are distributions acting on the initial densities. Since the root states are Schwartz distributions, both the observables and the initial densities should be smooth enough test functions.

We notice that the spectral decomposition (11) provides the asymptotic behavior of the mean value at arbitrarily long times  $t \rightarrow +\infty$ . Indeed, in the particular case where the real parts of the eigenvalues are ordered as

$$s_0 = 0 > \text{Re } s_1 \geq \text{Re } s_2 \geq \dots, \quad (12)$$

the leading eigenvalue  $s_0 = 0$  determines the limiting value of the mean value as

$$\lim_{t \rightarrow +\infty} \langle A \rangle_t = \langle A | \psi_0 \rangle \langle \tilde{\psi}_0 | \rho_0 \rangle, \quad (13)$$

while the next-to-leading eigenvalues determine the slowest relaxation modes toward the asymptotic stationary state. In the particular case where the eigenvalue  $s_0 = 0$  is unique and that Eq. (12) holds, the system is known to be ergodic and mixing [4].

The previous considerations show that the root states can be explicitly constructed by studying the asymptotic behavior of the mean value of an observable like (4) at arbitrarily long times  $t \rightarrow \infty$ . This asymptotic behavior provides the spectral decomposition of the Frobenius-Perron operator and, hence, of the Liouvillian operator, by identification of the terms in Eq. (11). This spectral decomposition is valid only for positive times  $t > 0$  and it therefore corresponds to the forward semigroup. We have used this method to construct the spectral decomposition of the Liouvillian operator near a pitchfork bifurcation in our previous work [8] and we shall here apply this method to the Hopf bifurcation.

Let us remark that a continuous spectrum of Liouvillian eigenvalues is expected when the dynamics presents power-law relaxations at criticality [8]. In this case, the spectral decomposition can also be constructed by studying the asymptotic time evolution of the mean value of an observable at  $t \rightarrow +\infty$ .

The past asymptotic behavior to  $t \rightarrow -\infty$  leads to another spectral decomposition corresponding to the backward semigroup.

### C. Trace formula

As long as we are interested in the eigenvalues, there exists a systematic method of calculation based on a trace formula for the Frobenius-Perron operator [2–4]. Indeed, if we defined the Frobenius-Perron operator by its spectral decomposition (10) in the biorthonormal basis (9), its trace would be given by

$$\text{Tr } \hat{P}^t = \text{Tr } e^{\hat{L}t} = \sum_j e^{s_j t} + 2 \sum_k e^{s_k t} + \dots, \quad (14)$$

where the first terms correspond to the nondegenerate eigenvalues, the second to the doubly degenerate eigenvalues, etc. This formal result shows that the trace of the Frobenius-Perron operator is a sum of decaying exponential functions in spite of the Jordan-block structure. This property allows us to identify the eigenvalues of the Liouvillian operator.

Now, the trace of the Frobenius-Perron operator can be calculated by noticing that its kernel is given by the Dirac-type distribution in Eq. (5). This distribution gives the conditional probability density to move from the initial point  $\mathbf{Y}$  to the final point  $\mathbf{X}$  during the time  $t$ . This conditional probability density is the analogue of the transition matrix

of a Markov chain for a continuous Markov-state space such as the phase space. In this perspective, we can define the trace of this transition probability density as

$$\text{Tr } \hat{P}^t = \text{Tr } e^{\hat{L}t} = \int \delta(\mathbf{X} - \Phi^t \mathbf{X}) d\mathbf{X} , \quad (15)$$

which is a definition independent of the coordinate system in phase space [2–4]. The contributions to the trace are given by the trajectories which return to their initial condition after a varying time  $t$  according to

$$\mathbf{X} = \Phi^t \mathbf{X} . \quad (16)$$

These closed solutions of the vector field are the stationary points,  $\mathbf{F}(\mathbf{X}_s) = 0$ , and the periodic orbits such that  $\mathbf{X}_p = \Phi^{rT_p} \mathbf{X}_p$  where  $T_p$  is the prime period and  $r = 1, 2, 3, \dots$  is the repetition number of the prime period. Both kinds of closed solutions contribute to the trace (15) as long as they are isolated, i.e., if they do not form continuous families. Otherwise, the integral of the Dirac distribution is not well defined in Eq. (15).

Previous works have emphasized the contribution of unstable and isolated periodic orbits which are dense in Axiom-A basic invariant sets such as the chaotic attractors and repellers [2, 3, 7]. However, stable periodic orbits as well as stationary points also contribute to the trace of the Frobenius-Perron operator, which is important in the case of a vector field with a Hopf bifurcation.

The trace of the Frobenius-Perron operator directly depends on the linear stability of the closed solutions, which we first assume to be hyperbolic, i.e., without marginal stability eigenvalue. The linear stability of a stationary point is characterized in terms of the vector field linearized near the stationary point

$$\delta \dot{\mathbf{X}} = \partial_{\mathbf{X}} \mathbf{F}(\mathbf{X}_s) \cdot \delta \mathbf{X} , \quad (17)$$

which has the solution

$$\delta \mathbf{X}_t = \exp \left[ \partial_{\mathbf{X}} \mathbf{F}(\mathbf{X}_s) t \right] \cdot \delta \mathbf{X}_0 . \quad (18)$$

The matrix of the linearized vector field has in general  $d$  eigenvalues  $\{\xi_{s,j}\}_{j=1}^d$ , which characterize the linear stability. The Lyapunov exponents of the stationary point are given by  $\lambda_{s,j} = \text{Re } \xi_{s,j}$ . None of them vanishes because of the assumed hyperbolicity.

The linear stability of a periodic orbit is characterized in terms of the linearized Poincaré map in a surface of section transverse to the periodic orbit. If we suppose that the phase-space variables separate into one variable  $X_{\parallel}$  parallel to the periodic orbit and  $(d-1)$  variables  $\mathbf{X}_{\perp}$  transverse to the periodic orbit, an infinitesimal perturbation of the periodic orbit is mapped after one period onto

$$\delta \mathbf{X}_{\perp, r+1} = \left[ \partial_{\mathbf{X}_{\perp}} \Phi_{\perp}^{T_p}(\mathbf{X}_p) \right] \cdot \delta \mathbf{X}_{\perp, r} \equiv \mathbf{m}_p \cdot \delta \mathbf{X}_{\perp, r} , \quad (19)$$

where  $\Phi_{\perp}$  is the transverse component of  $\Phi$  and we have introduced the  $(d-1) \times (d-1)$  matrix  $\mathbf{m}_p$  of the linearized Poincaré map. Its  $(d-1)$  eigenvalues  $\{\Lambda_{p,j}\}_{j=1}^{d-1}$  characterize the linear stability of the periodic orbit, which has the Lyapunov exponents  $\lambda_{p,j} = (1/T_p) \ln |\Lambda_{p,j}|$ . Here also, because of the assumed hyperbolicity, no Lyapunov exponent vanishes (except the one corresponding to the direction of the flow).

Using these results of linear-stability analysis in order to calculate the trace of the Frobenius-Perron operator, we obtain the trace formula

$$\begin{aligned} \text{Tr } \hat{P}^t = \text{Tr } e^{\hat{L}t} &= \sum_s \frac{1}{\left| \det \left\{ \mathbf{I} - \exp \left[ \partial_{\mathbf{X}} \mathbf{F}(\mathbf{X}_s) t \right] \right\} \right|} \\ &+ \sum_p \sum_{r=1}^{\infty} \frac{T_p \delta(t - rT_p)}{\left| \det \left\{ \mathbf{I} - \left[ \partial_{\mathbf{X}} \Phi_{\perp}^{T_p}(\mathbf{X}_p) \right]^r \right\} \right|} . \end{aligned} \quad (20)$$

This formula shows that the trace of the Frobenius-Perron operator diverges like

$$\text{Tr } \hat{P}^t \sim \frac{1}{|t|^d} , \quad \text{for } t \rightarrow 0 , \quad (21)$$

and that Dirac peaks appear at each positive repetition of each prime period. If we express the trace formula in terms of the stability eigenvalues of the stationary points and of the periodic orbits we obtain

$$\begin{aligned} \text{Tr } \hat{P}^t = \text{Tr } e^{\hat{L}t} &= \sum_s \sum_{\mathbf{l}, \mathbf{m}=0}^{\infty} \exp \left[ \sum_{\text{Re } \xi_{s,j} < 0} l_j \xi_{s,j} t - \sum_{\text{Re } \xi_{s,j} > 0} (m_j + 1) \xi_{s,j} t \right] \\ &+ \sum_p \sum_{r=1}^{\infty} T_p \delta(t - rT_p) \sum_{\mathbf{l}, \mathbf{m}=0}^{\infty} \left( \frac{\prod_{|\Lambda_{p,j}| < 1} \Lambda_{p,j}^{l_j}}{\prod_{|\Lambda_{p,j}| > 1} |\Lambda_{p,j}| \Lambda_{p,j}^{m_j}} \right)^r, \end{aligned} \quad (22)$$

for  $t > 0$ .

We observe that the Liouvillian eigenvalues associated with the basic invariant set formed by a stationary point are given by

$$\text{stationary point: } s_{\mathbf{l}\mathbf{m}} = \sum_{\text{Re } \xi_{s,j} < 0} l_j \xi_{s,j} - \sum_{\text{Re } \xi_{s,j} > 0} (m_j + 1) \xi_{s,j}, \quad (23)$$

with  $l_j, m_j = 0, 1, 2, 3, \dots$ . These resonances satisfy the relaxation condition  $\text{Re } s_{\mathbf{l}\mathbf{m}} \leq 0$  of the forward semigroup.

On the other hand, after a Laplace transform of Eq. (22) [2–4], we obtain the Liouvillian resonances associated with the basic invariant set formed by a single isolated periodic orbit as

$$\text{periodic orbit: } s_{\mathbf{l}\mathbf{m}\mathbf{n}} = \frac{1}{T_p} \left[ \sum_{|\Lambda_{p,j}| < 1} l_j \ln \Lambda_{p,j} - \sum_{|\Lambda_{p,j}| > 1} (\ln |\Lambda_{p,j}| + m_j \ln \Lambda_{p,j}) + 2\pi i n \right], \quad (24)$$

with  $l_j, m_j = 0, 1, 2, 3, \dots$  and  $n = 0, \pm 1, \pm 2, \pm 3, \dots$ . These resonances also satisfy the relaxation condition  $\text{Re } s_{\mathbf{l}\mathbf{m}\mathbf{n}} \leq 0$  of the forward semigroup.

Besides, the Liouvillian resonances associated with a chaotic basic invariant set in which there is a countable set of dense unstable periodic orbits are given by the zeros of a Selberg-Smale zeta function as shown elsewhere [2–4]. In the case of a single periodic orbit, the zeros of this zeta function are precisely the Liouvillian resonances given by Eq. (24).

The same method can also be used for isolated stationary points or periodic orbits of marginal stability as shown below for the Hopf bifurcation.

### III. THE HOPF BIFURCATION AND ITS LIOUVILLIAN RESONANCES

#### A. Hopf theorem

The Hopf bifurcation is a transition in which oscillations are born out of a stationary solution in a nonlinear dynamical system. This bifurcation has been much studied since the seminal work by Hopf [13]. A version of the theorem describing this bifurcation is provided by

*Theorem.* We suppose that the system (1) with  $\mathbf{X} \in \mathbb{R}^d$  and  $\mu \in \mathbb{R}$  has a stationary point which is put at the origin for convenience:  $\mathbf{X}_s(\mu) = 0$  for all  $\mu$ . The matrix  $\partial_{\mathbf{X}} \mathbf{F}(\mathbf{X}_s; \mu)$  of the linearized vector field at the critical parameter value  $\mu = 0$  is supposed to have a simple pair of pure imaginary eigenvalues,  $\xi_{\pm}(\mu = 0) = \pm i |\text{Im } \xi_{\pm}(\mu = 0)|$ , and all the other eigenvalues have a negative real part  $\text{Re } \xi_j(\mu = 0) < 0$  for  $j = 3, 4, \dots, d$ . Moreover, the pair of simple imaginary eigenvalues is supposed to satisfy

$$\frac{d}{d\mu} \text{Re } \xi_{\pm}(\mu = 0) \neq 0. \quad (25)$$

Then there is a unique center manifold passing through  $(\mathbf{X}_s = 0, \mu = 0)$  and a smooth system of coordinates for which the vector field has the form

$$\dot{z} = z (c_0 + c_2 |z|^2 + c_4 |z|^4 + \dots), \quad (26)$$

on the center manifold with  $z = x + iy$ . The Hopf bifurcation occurs at the critical parameter value  $\mu = 0$  where  $\text{Re } c_0 = 0$ .

If  $\text{Re } c_2 < 0$ , the stationary point is a stable focus for  $\text{Re } c_0 < 0$ . For  $\text{Re } c_0 > 0$ , the stationary point destabilizes into an unstable focus and gives birth to a stable periodic orbit. The Hopf bifurcation is said to be supercritical.

If  $\text{Re } c_2 > 0$ , the stationary point is a stable focus for  $\text{Re } c_0 < 0$  where it coexists with an unstable periodic orbit. At  $\text{Re } c_0 = 0$ , the unstable periodic orbit merges with the stationary point which becomes an unstable focus for  $\text{Re } c_0 > 0$ . In this case, the Hopf bifurcation is said to be subcritical.

If  $\text{Re } c_2 \neq 0$ , the radius of the periodic orbit vanishes like  $\sqrt{|\mu|}$  near the critical value  $\mu = 0$  where its period is

$$T(\mu = 0) = \frac{2\pi}{|\text{Im } \xi_{\pm}(\mu = 0)|} = \frac{2\pi}{|\text{Im } c_0(\mu = 0)|}. \quad (27)$$

See Refs. [1, 14–16].

We remark that the codimension-two case with  $\text{Re } c_2 = 0$  is a marginal situation connecting the supercritical and subcritical cases. Near such a codimension-two vector field, more than a single periodic orbit may exist. We shall here restrict ourselves to the study of the codimension-one Hopf bifurcation in the vicinity of the sole critical parameter value  $\mu = 0$  and of the bifurcating stationary point  $\mathbf{X}_s(\mu = 0)$ . Stationary points and periodic orbits outside this vicinity are ignored. Moreover, we notice that, in the subcritical case, the dynamics near the Hopf bifurcation is globally unstable since the trajectories escape from the phase-space region under study, unless  $\text{Re } c_0 < 0$  and the initial condition belongs to the basin of attraction of the stable focus. Therefore, we shall only study the supercritical case where an attractor exists throughout the bifurcation. The attractor is the stable focus before the bifurcation and the stable limit cycle after the bifurcation when the focus has become repelling.

The result that the vector field reduces to the two-dimensional vector field (26) in the sense of the center manifold theorem can be derived by the theory of normal forms [1, 15]. This result shows that the trajectories are attracted toward a two-dimensional center manifold on a transient time scale. After this transitory behavior which is not described by (26), the trajectories follow, on a long time scale, a nontrivial dynamics very close to the center manifold. The projection on the center manifold of this long-time dynamics is ruled by the vector field (26). Accordingly, we can restrict the study of the long-time dynamics of a Hopf bifurcation to the study of the vector field (26).

After an appropriate rescaling of the parameters, we can set

$$c_0 \equiv \mu + i \omega, \quad (28)$$

$$c_2 \equiv -\alpha - i \beta = -1 - i \beta. \quad (29)$$

The last equality is obtained after a rescaling of the phase-space variables under our assumption that the Hopf bifurcation is supercritical so that  $\alpha > 0$ .

Introducing polar coordinates

$$z = x + i y = r \exp(i\theta), \quad (30)$$

the vector field (26) becomes

$$\begin{cases} \dot{r} = r [\mu - r^2 + \mathcal{O}(r^4)], \\ \dot{\theta} = \omega - \beta r^2 + \mathcal{O}(r^4). \end{cases} \quad (31)$$

The linearized radial equation is

$$\delta \dot{r} = [\mu - 3r^2 + \mathcal{O}(r^4)] \delta r. \quad (32)$$

Consequently, the focus at the origin  $r = 0$  has the stability eigenvalues:

$$\text{focus: } \xi_{\pm} = \mu \pm i \omega, \quad (33)$$

so that the focus is stable if  $\mu < 0$  and unstable if  $\mu > 0$ .

On the other hand, the periodic orbit exists at the radius

$$\text{periodic orbit: } r_p = \sqrt{\mu} + \mathcal{O}(\mu^{3/2}), \quad \text{if } \mu > 0. \quad (34)$$

Inserting this radius in the angular equation of Eqs. (31), we infer that the periodic orbit has the period

$$T(\mu) = \frac{2\pi}{|\omega - \beta\mu + \mathcal{O}(\mu^2)|}, \quad (35)$$

and the Lyapunov exponent

$$\lambda(\mu) = \frac{1}{T(\mu)} \ln |\Lambda(\mu)| = -2\mu + \mathcal{O}(\mu^2), \quad (36)$$

corresponding to a positive stability eigenvalue  $0 < \Lambda(\mu) < 1$ . Typical phase portraits of the vector field (31) are depicted in Fig. 1.

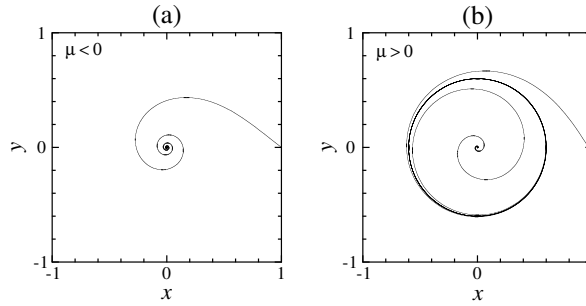


FIG. 1: Typical phase portraits of a two-dimensional system undergoing a Hopf bifurcation: (a) before criticality for  $\mu < 0$ ; (b) after criticality for  $\mu > 0$ .

### B. The Liouvillian operator

The Liouvillian operator of a vector field undergoing the Hopf bifurcation can be written in polar coordinates. If the equations of motion are

$$\begin{cases} \dot{r} = r f(r), \\ \dot{\theta} = g(r), \end{cases} \quad (37)$$

the Liouvillian operator is

$$\hat{L} \rho = -\frac{1}{r} \frac{\partial}{\partial r} [r^2 f(r) \rho] - g(r) \frac{\partial \rho}{\partial \theta}, \quad (38)$$

while its adjoint is

$$\hat{L}^\dagger \rho = +r f(r) \frac{\partial \rho}{\partial r} + g(r) \frac{\partial \rho}{\partial \theta}, \quad (39)$$

so that

$$\hat{L} + \hat{L}^\dagger = -\left[2f(r) + r \frac{df(r)}{dr}\right] \hat{I}. \quad (40)$$

### C. The Liouvillian resonances

The general theory of the trace formula presented in Section II provides the spectrum of the Liouvillian operator using the results of the linear stability analysis of the stationary point and the limit cycle.

The trace of the Frobenius-Perron operator of the vector field (31) is given by

$$\mu < 0 : \quad \text{Tr } \hat{P}^t = \frac{1}{|1 - 2 \exp(\mu t) \cos \omega t + \exp(2\mu t)|}, \quad (41)$$

before the bifurcation when there only exists the stationary point. When the limit cycle is born, the trace of the Frobenius-Perron operator becomes

$$\mu > 0 : \quad \text{Tr } \hat{P}^t = \frac{1}{|1 - 2 \exp(\mu t) \cos \omega t + \exp(2\mu t)|} + \sum_{r=1}^{\infty} \frac{T(\mu)}{|1 - \Lambda(\mu)^r|} \delta[t - rT(\mu)], \quad (42)$$

with the periodic-orbit contribution for  $t > 0$ .

Accordingly, the Liouvillian resonances of the forward semigroup are given by

$$\mu < 0 : \quad \text{stable focus: } s_{l_+ l_-} = (l_+ + l_-) \mu + i(l_+ - l_-) \omega, \quad (43)$$

with  $l_{\pm} = 0, 1, 2, 3, \dots$ . Therefore, the spectrum forms a pyramidal array of resonances before the bifurcation, as depicted in Fig. 2.



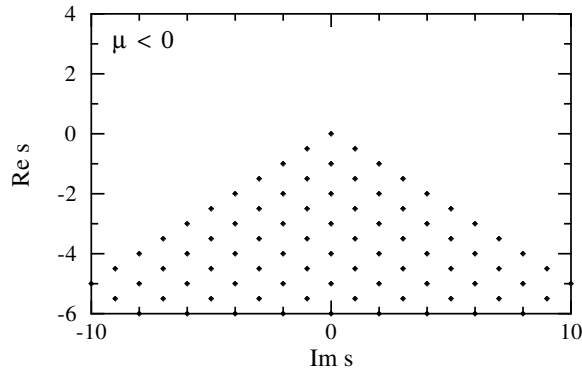


FIG. 2: Typical spectrum of Liouvillian resonances  $s \in \mathbb{C}$  before criticality ( $\mu < 0$ ).

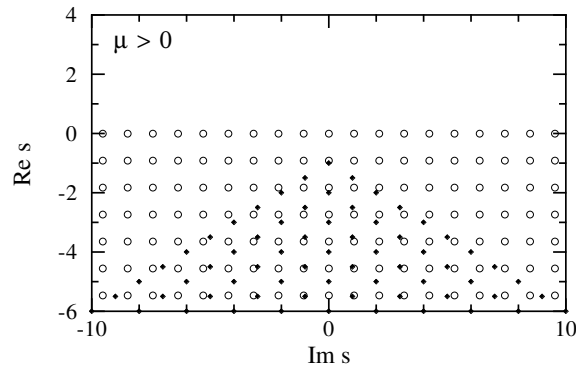


FIG. 3: Typical spectrum of Liouvillian resonances  $s \in \mathbb{C}$  after criticality ( $\mu > 0$ ). The filled circles are the resonances associated with the unstable focus, while the open circles are those associated with the limit cycle.

After the bifurcation, the resonances become

$$\begin{aligned}
 \mu > 0 : \quad \text{unstable focus: } s_{m_+ m_-}^{(f)} &= -(m_+ + m_- + 2) \mu - i (m_+ - m_-) \omega ; \\
 \text{limit cycle: } s_{ln}^{(c)} &= \frac{1}{T(\mu)} \left[ l \ln |\Lambda(\mu)| + 2\pi i n \right] \\
 &= l \left[ -2\mu + \mathcal{O}(\mu^2) \right] + i n \left[ \omega - \beta\mu + \mathcal{O}(\mu^2) \right] , \quad (44)
 \end{aligned}$$

with  $m_{\pm}, l = 0, 1, 2, 3, \dots$  and  $n = 0, \pm 1, \pm 2, \pm 3, \dots$ . The spectrum is now composed of a half-lattice of resonances due to the limit cycle together with a pyramidal array of resonances due to the unstable focus (see Fig. 3). The resonances of the limit cycle with  $l = 0$  have a vanishing real part so that  $\text{Re } s = 0$  and they control the long-time oscillations of the system. These resonances with a vanishing relaxation rate are the Koopman eigenvalues of the Liouvillian operator.

In the following section, we shall obtain the eigenstates and other root states associated with the generalized eigenvalues (43)-(44) of the Liouvillian operator.

## IV. THE HOPF BIFURCATION AND ITS SPECTRAL DECOMPOSITION

### A. The vector field and its Liouvillian operator

Our purpose is here to obtain the full spectral decomposition of the Liouvillian dynamics of the Hopf bifurcation. We have already calculated the resonances, i.e., the generalized eigenvalues. In the present section, we shall construct the corresponding eigenstates and other root states.

Here, we consider the vector field with the nonlinear terms responsible for the Hopf bifurcation in the following truncated cubic form

$$\dot{z} = (\mu + i\omega) z - (1 + i\beta) |z|^2 z, \quad (45)$$

where  $\mu$  is the bifurcation parameter. In the polar coordinates  $z = r \exp(i\theta)$ , the vector field becomes

$$\begin{cases} \dot{r} = \mu r - r^3, \\ \dot{\theta} = \omega - \beta r^2. \end{cases} \quad (46)$$

The Hopf bifurcation occurs at the critical parameter value  $\mu = 0$ . Before the bifurcation ( $\mu < 0$ ), the stationary point at the origin is a stable focus, which becomes unstable after the bifurcation ( $\mu > 0$ ). At criticality ( $\mu = 0$ ), a limit cycle is born with a radius  $r = \sqrt{\mu}$ .

As we explained in Sec. II, the time evolution of the average of an observable can be calculated if we know the flow (2) of the system. In the case of the vector field (46), the equations can be integrated to get the following flow

$$\begin{aligned} \Phi^t : \quad r_t &= r_0 \sqrt{\frac{\mu}{r_0^2 + (\mu - r_0^2) \exp(-2\mu t)}}, \\ \theta_t &= \theta_0 + (\omega - \mu\beta)t + \beta \ln \sqrt{\frac{\mu}{r_0^2 + (\mu - r_0^2) \exp(-2\mu t)}}. \end{aligned} \quad (47)$$

For a fixed initial condition at radial distance  $r_0$ , Eqs. (47) hold for times larger than a critical negative time at which the trajectory diverges to infinity

$$t > t_c = -\frac{1}{2\mu} \ln \frac{r_0^2}{r_0^2 - \mu} < 0. \quad (48)$$

This critical time  $t_c$  exists for all values of  $r_0$  before the bifurcation  $\mu < 0$ , and for trajectories exterior to the limit cycle with  $r_0 > \sqrt{\mu}$  after the bifurcation  $\mu > 0$ . For the trajectories inside the limit cycle with  $r_0 < \sqrt{\mu}$ , Eqs. (47) hold at all times. The divergence of the trajectories at the negative time  $t_c$  is due to the cubic term in the vector field. Since we are here interested in the forward semigroup which applies at positive times  $t > 0$  we shall always work within the domain of validity (48) of Eqs. (47).

The inverse of the flow (47) is given by

$$\begin{aligned} \Phi^{-t} : \quad r_0 &= r_t \sqrt{\frac{\mu}{r_t^2 + (\mu - r_t^2) \exp(2\mu t)}}, \\ \theta_0 &= \theta_t - (\omega - \beta\mu)t + \beta \ln \sqrt{\frac{\mu}{r_t^2 + (\mu - r_t^2) \exp(2\mu t)}}. \end{aligned} \quad (49)$$

The Jacobian of the transformation is

$$r_0 dr_0 d\theta_0 = \frac{e^{-2\mu t}}{[1 + r_t^2(e^{-2\mu t} - 1)/\mu]^2} r_t dr_t d\theta_t. \quad (50)$$

Thanks to Eqs. (47), we can calculate the time evolution of the average of an observable and, consequently, obtain the spectral decomposition of the Liouvillian operator which is here given by

$$\frac{\partial \rho}{\partial t} = \hat{L} \rho = -\frac{1}{r} \frac{\partial}{\partial r} [r^2(\mu - r^2)\rho] - (\omega - \beta r^2) \frac{\partial \rho}{\partial \theta}. \quad (51)$$

In order to obtain the spectral decomposition of the Liouvillian operator, we consider the time evolution of the mean value of an observable (4), which is given by

$$\langle A \rangle_t = \int dr r d\theta \rho(r, \theta) A[\Phi^t(r, \theta)], \quad (52)$$

with  $r = r_0$  and  $\theta = \theta_0$  and where we used  $dx dy = r dr d\theta$ . In Eq. (52),  $\rho$  denotes the density of initial conditions and  $A$  the observable. Moreover, we introduce the inner product

$$\langle \phi | \psi \rangle \equiv \int_0^\infty dr r \int_0^{2\pi} d\theta \phi^*(r, \theta) \psi(r, \theta). \quad (53)$$

## B. Fourier series

In polar coordinates, both the observable and the initial density are periodic functions in the angle  $\theta$  of period  $2\pi$ . Accordingly, these functions can be expanded in Fourier series:

$$A(r, \theta) = \frac{1}{\sqrt{2\pi}} \sum_{n=-\infty}^{+\infty} A_n(r) e^{+in\theta}, \quad (54)$$

$$A_n(r) = \int_0^{2\pi} \frac{d\theta}{\sqrt{2\pi}} e^{-in\theta} A(r, \theta), \quad (55)$$

$$\rho(r, \theta) = \frac{1}{\sqrt{2\pi}} \sum_{n=-\infty}^{+\infty} \rho_n(r) e^{+in\theta}, \quad (56)$$

$$\rho_n(r) = \int_0^{2\pi} \frac{d\theta}{\sqrt{2\pi}} e^{-in\theta} \rho(r, \theta), \quad (57)$$

and the coefficients of the Fourier series are functions of  $r$  satisfying

$$A_{-n}(r) = A_n^*(r), \quad \text{and} \quad \rho_{-n}(r) = \rho_n^*(r). \quad (58)$$

If we assume that the observable or the density is a function which is analytic in each of the Cartesian variables  $x$  and  $y$ , we notice that the coefficients of order  $n$  of the Fourier series behave as

$$A(x, y) \text{ analytic} \implies A_n(r) = r^{|n|} f_n(r^2), \quad (59)$$

$$\rho(x, y) \text{ analytic} \implies \rho_n(r) = r^{|n|} g_n(r^2), \quad (60)$$

where  $f_n$  and  $g_n$  are analytic functions of  $r^2$ .

In the following, we shall treat separately the spectral decomposition in the subcritical ( $\mu < 0$ ), the critical ( $\mu = 0$ ), and the supercritical ( $\mu > 0$ ) regimes.

## C. The subcritical regime: $\mu < 0$

In the subcritical regime, the vector field (46) has no periodic orbit but a unique stationary point which is a stable focus. In order to obtain the spectral decomposition (10) of the Frobenius-Perron operator, we study the asymptotic behavior of the mean value (52) at long positive times, by performing a Taylor expansion in the small quantity  $\exp(-|\mu|t)$  which vanishes for  $t \rightarrow +\infty$ . This asymptotic expansion should allow us to identify the eigenstates and other root states thanks to Eq. (11).

With this aim, we start from Eq. (52) for the mean value of an observable, with the flow given by Eqs. (47). Since both the observable and the initial density are periodic in the angle  $\theta$ , we expand them in Fourier series according to Eqs. (54) and (56). After integration over the angle  $\theta$ , we get

$$\begin{aligned} \langle A \rangle_t = & \sum_{n=-\infty}^{+\infty} e^{-in\omega t} \int_0^\infty dr \ r \left( 1 + \frac{r^2}{|\mu|} - \frac{r^2}{|\mu|} e^{-2|\mu|t} \right)^{in\beta/2} \rho_n(r) \\ & \times A_n^* \left( \frac{r e^{-|\mu|t}}{\sqrt{1 + \frac{r^2}{|\mu|} - \frac{r^2}{|\mu|} e^{-2|\mu|t}}} \right). \end{aligned} \quad (61)$$

In the limit  $t \rightarrow +\infty$ , the quantity  $\exp(-|\mu|t)$  decays to zero so that the spectral decomposition into decaying exponentials can be obtained by a Taylor expansion of this quantity. However, we notice that this quantity appears in the group

$$\xi \equiv \frac{r e^{-|\mu|t}}{\sqrt{|\mu| + r^2}}, \quad (62)$$

in Eq. (61). Therefore, we can equivalently perform the Taylor expansion in terms of this new variable  $\xi$ .

Substituting (62) into Eq. (61), we get

$$\langle A \rangle_t = \sum_{n=-\infty}^{+\infty} e^{-in\omega t} \int_0^{\infty} dr r \left(1 + \frac{r^2}{|\mu|}\right)^{in\beta/2} \rho_n(r) (1 - \xi^2)^{in\beta/2} A_n^* \left( \frac{\xi \sqrt{|\mu|}}{\sqrt{1 - \xi^2}} \right). \quad (63)$$

A Taylor expansion is performed with respect to the variable  $\xi$  around its limit  $\xi = 0^+$  for  $t \rightarrow +\infty$

$$(1 - \xi^2)^{in\beta/2} A_n^* \left( \frac{\xi \sqrt{|\mu|}}{\sqrt{1 - \xi^2}} \right) = \sum_{l=0}^{\infty} \frac{\xi^l}{l!} \frac{\partial^l}{\partial \xi^l} \left[ (1 - \xi^2)^{in\beta/2} A_n^* \left( \frac{\xi \sqrt{|\mu|}}{\sqrt{1 - \xi^2}} \right) \right]_{\xi=0^+}. \quad (64)$$

Replacing in Eq. (63), the series in powers of  $\xi^l$  gives us the different terms corresponding to the different exponential relaxations  $\exp(-l|\mu|t)$ . Whereupon, we finally obtain the spectral decomposition

$$\langle A \rangle_t = \sum_{l=0}^{\infty} \sum_{n=-l}^{+l} \langle A | \psi_{ln} \rangle e^{s_{ln} t} \langle \tilde{\psi}_{ln} | \rho \rangle, \quad (65)$$

with the expected generalized eigenvalues

$$s_{ln} = -l |\mu| - i n \omega, \quad l = 0, 1, 2, 3, \dots, \quad n = -l, -l + 2, \dots, +l - 2, +l, \quad (66)$$

and the coefficients

$$\begin{aligned} \langle A | \psi_{ln} \rangle &= \frac{1}{l!} \frac{\partial^l}{\partial \xi^l} \left[ (1 - \xi^2)^{in\beta/2} A_n^* \left( \frac{\xi \sqrt{|\mu|}}{\sqrt{1 - \xi^2}} \right) \right]_{\xi=0^+}, \\ \langle \tilde{\psi}_{ln} | \rho \rangle &= \int_0^{\infty} dr r \frac{(r/\sqrt{|\mu|})^l}{(1 + r^2/|\mu|)^{(l-in\beta)/2}} \rho_n(r). \end{aligned} \quad (67)$$

We notice that the integer  $n$  is restricted to the values ranging from  $-l$  to  $+l$  by steps of 2, hence the restricted sum  $\sum'$  in Eq. (65). The vanishing of the other terms has its origin in the fact that the observable  $A$  is supposed to be analytic near the origin in the Cartesian coordinates  $(x, y)$ , or equivalently of  $(z, z^*)$ .

Using the definitions of the Fourier coefficients (55) and (57), as well as the inner product (53), we can obtain the explicit expression for the right and left eigenstates in terms of their integral kernels as

$$\begin{aligned} \psi_{ln}(r, \theta) &= \frac{\exp(in\theta)}{\sqrt{2\pi}} \frac{1}{l!} \frac{\partial^l}{\partial \xi^l} \left[ (1 - \xi^2)^{in\beta/2} \frac{1}{r} \delta \left( r - \frac{\xi \sqrt{|\mu|}}{\sqrt{1 - \xi^2}} \right) \right]_{\xi=0^+}, \\ \tilde{\psi}_{ln}(r, \theta) &= \frac{\exp(in\theta)}{\sqrt{2\pi}} \frac{(r/\sqrt{|\mu|})^l}{(1 + r^2/|\mu|)^{(l+in\beta)/2}}. \end{aligned} \quad (68)$$

These eigenstates are biorthonormal

$$\langle \tilde{\psi}_{ln} | \psi_{l'n'} \rangle = \delta_{ll'} \delta_{nn'}. \quad (69)$$

We can verify that the kernels (68) are the eigenstates of the Liouvillian operator (51) associated with the eigenvalues (66) in the sense that:

$$\mu < 0 : \quad \hat{L} \psi_{ln} = s_{ln} \psi_{ln}, \quad (70)$$

$$\hat{L}^\dagger \tilde{\psi}_{ln} = s_{ln}^* \tilde{\psi}_{ln}. \quad (71)$$

The first line is checked by applying a smooth enough test function  $A(r, \theta)$  to both members of the equation. The second line is checked by a direct calculation.

As aforementioned, the assumption of analyticity of the observables implies that most of the coefficients of the Fourier series of  $A$  vanish at  $r = 0$ , except those with  $n = -l, -l + 2, \dots, +l - 2, +l$ . As a consequence, the eigenvalues (66) form a pyramidal array in the plane of the complex variable  $s$ , as depicted in Fig. 2. The pyramidal array is the signature of the stable focus existing before the Hopf bifurcation. Indeed, in the subcritical regime, this stationary point is the attractor around which the oscillations are damped. The oscillations can be decomposed by the Fourier analysis into their harmonics. It turns out that the relaxation rate of the harmonics increases with their frequency. As a consequence, the relaxation of the oscillations creates a pyramidal array of Liouvillian resonances. We notice that, as the criticality is approached, the relaxation rates decrease so that the pyramidal array becomes wider and wider because the resonances approach the imaginary axis. Near criticality, the real spacing between the resonances also decreases because the damping decreases, so that the resonances accumulate into lines, as shown below.

### D. The critical regime: $\mu = 0$

At criticality, the stationary point becomes a slowly attracting focus. The equations (46) can be integrated and the flow (47) becomes

$$\begin{aligned} \Phi^t : \quad r_t &= \frac{r_0}{\sqrt{1 + 2r_0^2 t}}, \\ \theta_t &= \theta_0 + \omega t - \beta \ln \sqrt{1 + 2r_0^2 t}, \end{aligned} \quad (72)$$

which holds for

$$t > t_c = -\frac{1}{2r_0^2} < 0, \quad (73)$$

and, thus, for our purpose to derive a forward semigroup valid for positive times  $t > 0$ . We observe that the radial position relaxes to zero according to the power law  $r_t \sim 1/\sqrt{t}$ , although this relaxation was exponential in the subcritical case. This slow dynamics is a characteristic feature of critical systems at bifurcations and it is referred to as a *critical slowing down*.

As in Sec. IV C, we calculate the time evolution of the average value of an observable by substituting the critical flow (72) in Eq. (52). By using the Fourier series (54) and (56), we get

$$\langle A \rangle_t = \sum_{n=-\infty}^{+\infty} e^{-in\omega t} \int_0^\infty dr r \rho_n(r) A_n^* \left( \frac{r}{\sqrt{1 + 2r^2 t}} \right) (1 + 2r^2 t)^{in\beta/2}. \quad (74)$$

Since the argument of the functions  $A_n^*$  tends to zero in the limit  $t \rightarrow +\infty$ , we perform the following Taylor expansion

$$A_n^* \left( \frac{r}{\sqrt{1 + 2r^2 t}} \right) = A_n^*(0) + \sum_{l=1}^{\infty} \frac{A_n^{*(l)}(0)}{l!} \frac{r^l}{(1 + 2r^2 t)^{l/2}}, \quad (75)$$

where  $A_n^{*(l)}(r)$  denotes the  $l^{\text{th}}$  derivative of  $A_n^*(r)$ . Here we assume the analyticity of the observable  $A(x, y)$  in each variables  $x$  and  $y$  so that

$$A_n^*(0) = 0, \quad \text{for } n \neq 0, \quad (76)$$

according to the property (59). Moreover, we use the following integral representation

$$\frac{r^l}{(1 + 2r^2 t)^{(l-i\beta n)/2}} = \frac{r^{l-2}}{2\Gamma\left(\frac{l-i\beta n}{2}\right)} \int_{-\infty}^0 d\sigma \exp(\sigma t) \left(-\frac{\sigma}{2r^2}\right)^{\frac{l-i\beta n-2}{2}} \exp\left(\frac{\sigma}{2r^2}\right). \quad (77)$$

This formula shows that the spectrum of relaxation rates is continuous at criticality, although it is discrete away from criticality.

Substituting the results (75), (76) and (77) into the expansion (74), we obtain finally the spectral decomposition

$$\langle A \rangle_t = \langle A|\psi_0\rangle \langle \tilde{\psi}_0|\rho\rangle + \sum_{n=-\infty}^{+\infty} \int_{-\infty}^0 d\sigma \langle A|\psi_{\sigma n}\rangle e^{(\sigma-in\omega)t} \langle \tilde{\psi}_{\sigma n}|\rho\rangle, \quad (78)$$

with the coefficients

$$\begin{aligned} \langle A|\psi_0\rangle &= A_0^*(0), \\ \langle \tilde{\psi}_0|\rho\rangle &= \int_0^\infty dr r \rho_0(r), \\ \langle A|\psi_{\sigma n}\rangle &= \sum_{l=1}^{\infty} \frac{A_n^{*(l)}(0)}{2 l! \Gamma\left(\frac{l-i\beta n}{2}\right)} \left(-\frac{\sigma}{2}\right)^{\frac{l-i\beta n-2}{2}}, \\ \langle \tilde{\psi}_{\sigma n}|\rho\rangle &= \int_0^\infty dr r^{1+i\beta n} \exp\left(\frac{\sigma}{2r^2}\right) \rho_n(r). \end{aligned} \quad (79)$$

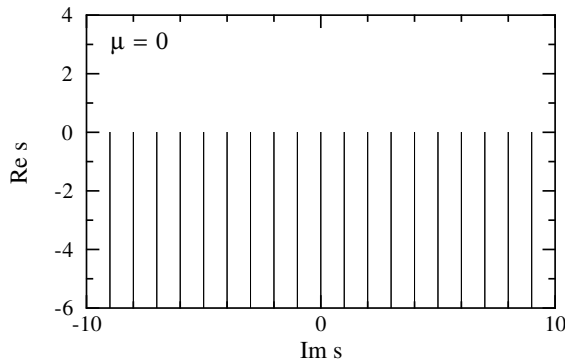


FIG. 4: Continuous spectrum of the spectral decomposition (78) of the cubic vector field (46) at criticality ( $\mu = 0$ ).

With the definitions of the Fourier coefficients (55) and (57) and of the inner product (53), the kernels of the right and left eigenstates can be obtained as

$$\begin{aligned}
 \psi_0(r, \theta) &= \frac{1}{\sqrt{2\pi}} \left[ \frac{\delta(r-R)}{r} \right]_{R=0^+}, \\
 \tilde{\psi}_0(r, \theta) &= \frac{1}{\sqrt{2\pi}}, \\
 \psi_{\sigma n}(r, \theta) &= \frac{\exp(in\theta)}{\sqrt{2\pi}} \sum_{l=1}^{\infty} \frac{1}{2 \, l! \, \Gamma\left(\frac{l-i\beta n}{2}\right)} \left(-\frac{\sigma}{2}\right)^{\frac{l-i\beta n-2}{2}} \left[ \frac{\partial^l}{\partial R^l} \frac{\delta(r-R)}{r} \right]_{R=0^+}, \\
 \tilde{\psi}_{\sigma n}(r, \theta) &= \frac{\exp(in\theta)}{\sqrt{2\pi}} r^{-i\beta n} \exp\left(\frac{\sigma}{2r^2}\right).
 \end{aligned} \tag{80}$$

The kernels (80) can be verified to be the eigenstates of the Liouvillian operator (51) with  $\mu = 0$  associated with the generalized eigenvalue  $s = \sigma - in\omega$ .

As aforementioned, the spectrum is here continuous and extends from  $s = in\omega$  to  $s = in\omega - \infty$  with  $n = 0, \pm 1, \pm 2, \pm 3, \dots$  (see Fig. 4). Consequently, the spectral decomposition is expressed as an integral over the continuous relaxation rate  $|\sigma|$ , instead of a discrete sum over a discrete spectrum of resonances. Accordingly, the coefficients of the spectral decomposition also depend on the continuous relaxation rate  $|\sigma|$ .

The continuous character of the Liouvillian spectrum directly implies that the time evolution obeys a power-law relaxation at criticality. The power-law relaxation of the average  $\langle A \rangle_t$  to the stationary value easily follows from the spectral decomposition (78) and (79). Indeed, because of (79), we have for small  $|\sigma|$

$$\langle A | \psi_{\sigma n} \rangle \sim \frac{1}{\sqrt{|\sigma|}} e^{-in\beta \ln \sqrt{|\sigma|}} \quad \langle \tilde{\psi}_{\sigma n} | \rho \rangle \sim \text{constant}, \tag{81}$$

and, because of the Abelian theorem for the Laplace transform [26], we have

$$\int_{-\infty}^0 d\sigma \langle A | \psi_{\sigma n} \rangle e^{(\sigma - in\omega)t} \langle \tilde{\psi}_{\sigma n} | \rho \rangle \sim \frac{1}{\sqrt{t}} e^{-in(\omega t - \beta \ln \sqrt{t})}. \tag{82}$$

The next terms of the asymptotic series decay as  $1/\sqrt{t^l}$  with  $l = 2, 3, \dots$ , multiplied by the oscillating factor. The leading term with  $n = 0$  decays as  $1/\sqrt{t}$ . Therefore, the statistical average  $\langle A \rangle_t$  relaxes to its stationary value according to the power law  $1/\sqrt{t}$ .

We notice that the continuous Liouvillian spectrum is caused by the critical slowing down of the amplitude of the oscillations at the Hopf bifurcation, as described by Eq. (72). Moreover, the continuous spectrum has for consequence that the probability densities and the statistical averages ruled by the Frobenius-Perron operator have power-law relaxation as  $1/\sqrt{t}$  in the long time limit  $t \rightarrow \infty$ . We can understand this power-law relaxation by the collapse into a continuous spectrum of the numerous resonances existing before and after the Hopf bifurcation (see Secs. IVC and IVE). Indeed, away from the bifurcation, the spectrum is discrete and each resonance corresponds to an exponential

relaxation. Under such circumstances, the statistical averages are given by the sum of many exponential functions of time. When the resonances collapse into a continuous spectrum at criticality, the sum of many exponential functions with distributed relaxation rates turns into an asymptotic power-law behavior at long times, which explains the power-law relaxation of statistical averages occurring at the Hopf bifurcation.

### E. The supercritical regime: $\mu > 0$

In the supercritical regime, the vector field (46) has an unstable focus at  $r = 0$  with the stability eigenvalues  $\mu \pm i\omega$  and a periodic orbit (limit cycle) at  $r = \sqrt{\mu}$  with the Lyapunov exponent  $\lambda = -2\mu$ . The phase space  $(r, \theta)$  separates into two domains:

$$\text{the exterior domain :} \quad \sqrt{\mu} \leq r < \infty ; \quad (83)$$

$$\text{the interior domain :} \quad 0 \leq r < \sqrt{\mu} . \quad (84)$$

The first domain is exterior to the limit cycle while the second is interior. The average of an observable can be decomposed into two terms, one corresponding to each domain:

$$\langle A \rangle_t = \langle A \rangle_t^{\text{ex}} + \langle A \rangle_t^{\text{in}} . \quad (85)$$

The domains (83)-(84) will be treated separately. The exterior domain will be treated before the interior domain because its treatment is easier.

#### 1. The exterior domain

The exterior domain is easier because it contains a single closed solution of the flow, namely, the limit cycle which is the boundary of the exterior domain.

For the flow given by Eq. (47), we calculate the time evolution of the mean value (52) of an observable. We expand the observable and the initial density in Fourier series of the angle  $\theta$  according to Eqs. (54) and (56) and we integrate over the angle to get

$$\langle A \rangle_t^{\text{ex}} = \sum_{n=-\infty}^{+\infty} e^{-in(\omega-\mu\beta)t} \int_{\sqrt{\mu}}^{\infty} dr r \left( \frac{r}{\sqrt{\mu}} \right)^{in\beta} \rho_n(r) (1+\zeta)^{in\beta/2} A_n^* \left( \sqrt{\frac{\mu}{1+\zeta}} \right), \quad (86)$$

where we have introduced

$$\zeta \equiv \left( \frac{\mu}{r^2} - 1 \right) e^{-2\mu t} . \quad (87)$$

This quantity decays to zero in the limit  $t \rightarrow +\infty$  so that the spectral decomposition into decaying exponentials can be obtained by a Taylor expansion in powers of the quantity (87) as

$$(1+\zeta)^{in\beta/2} A_n^* \left( \sqrt{\frac{\mu}{1+\zeta}} \right) = \sum_{l=0}^{\infty} \frac{\zeta^l}{l!} \frac{\partial^l}{\partial \zeta^l} \left[ (1+\zeta)^{in\beta/2} A_n^* \left( \sqrt{\frac{\mu}{1+\zeta}} \right) \right]_{\zeta=0} . \quad (88)$$

Substituting the results (88) into the expression (86), we obtain the decomposition

$$\langle A \rangle_t^{\text{ex}} = \sum_{n=-\infty}^{+\infty} \sum_{l=0}^{\infty} \langle A | \psi_{ln}^{\text{ex}(c)} \rangle e^{s_{ln}^{(c)} t} \langle \tilde{\psi}_{ln}^{\text{ex}(c)} | \rho \rangle , \quad (89)$$

with the generalized eigenvalues

$$s_{ln}^{(c)} = -2l\mu - in(\omega - \mu\beta), \quad l = 0, 1, 2, 3, \dots, \quad n = 0, \pm 1, \pm 2, \pm 3, \dots, \quad (90)$$

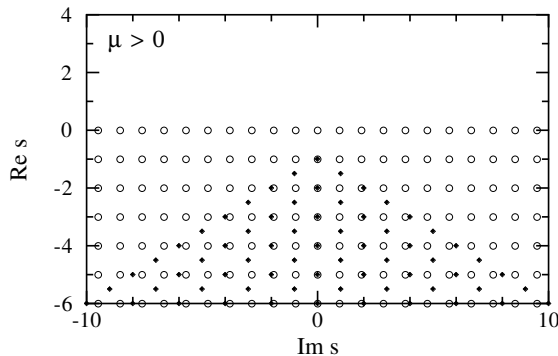


FIG. 5: Spectrum (93)-(94) of the Liouvillian resonances  $s \in \mathbb{C}$  of the cubic vector field (46) after criticality ( $\mu > 0$ ). Notice the degeneracies for the resonances on  $\text{Im } s = 0$ . The filled circles are the resonances associated with the unstable focus, while the open circles are those associated with the limit cycle.

and the coefficients

$$\begin{aligned} \langle A | \psi_{ln}^{\text{ex}(c)} \rangle &= \frac{1}{l!} \frac{\partial^l}{\partial \zeta^l} \left[ (1 + \zeta)^{in\beta/2} A_n^* \left( \sqrt{\frac{\mu}{1 + \zeta}} \right) \right]_{\zeta=0^-}, \\ \langle \tilde{\psi}_{ln}^{\text{ex}(c)} | \rho \rangle &= \int_{\sqrt{\mu}}^{\infty} dr r \left( \frac{r}{\sqrt{\mu}} \right)^{in\beta} \left( \frac{\mu}{r^2} - 1 \right)^l \rho_n(r). \end{aligned} \quad (91)$$

In the present supercritical case, the integers  $l$  and  $n$  have no constraint because  $A_n^*$  is here evaluated on the limit cycle at  $r = \sqrt{\mu} \neq 0$  so that the analyticity condition at  $r = 0$  plays no role here. As a consequence, the resonances associated with the external side of the limit cycle form a half-lattice.

By the definitions of the Fourier coefficients (55) and (57) and of the inner product (53), the right and left eigenstates can be explicitly expressed in terms of their integral kernels as

$$\begin{aligned} \psi_{ln}^{\text{ex}(c)}(r, \theta) &= \frac{\exp(in\theta)}{\sqrt{2\pi}} \frac{1}{l!} \frac{\partial^l}{\partial \zeta^l} \left[ (1 + \zeta)^{in\beta/2} \frac{1}{r} \delta \left( r - \sqrt{\frac{\mu}{1 + \zeta}} \right) \right]_{\zeta=0^-}, \\ \tilde{\psi}_{ln}^{\text{ex}(c)}(r, \theta) &= \frac{\exp(in\theta)}{\sqrt{2\pi}} \left( \frac{r}{\sqrt{\mu}} \right)^{-in\beta} \left( \frac{\mu}{r^2} - 1 \right)^l \theta(r - \sqrt{\mu}), \end{aligned} \quad (92)$$

where  $\theta(r - \sqrt{\mu})$  denotes the Heaviside function which is the characteristic function of the exterior domain.

## 2. The interior domain

The interior domain has the stable limit cycle for its boundary  $r = \sqrt{\mu}$  and contains the unstable focus at  $r = 0$ . We may expect that the dynamics on the internal side of the limit cycle also produces the half-lattice of the resonances (90). Furthermore, we also find the resonances associated with the unstable focus [cf. Eq. (44)]. The expected resonances are thus:

$$\text{stable cycle : } s_{ln}^{(c)} = -2l\mu - in(\omega - \mu\beta), \quad \text{with } l \in \mathbb{N} \ \& \ n \in \mathbb{Z}, \quad (93)$$

$$\begin{aligned} \text{unstable focus : } s_{mn}^{(f)} &= -(m+2)\mu - in\omega, \quad \text{with } m \in \mathbb{N} \\ &\ \& \ n = -m, -m+2, \dots, m-2, m. \end{aligned} \quad (94)$$

This spectrum is depicted in Fig. 5.

We observe in Fig. 5 that the resonances of the limit cycle coincide with those of the unstable focus if  $n = 0$  because these resonances are integer multiples of  $-\mu$ , as shown by Eqs (93) and (94). This degeneracy of the resonance spectrum leads to the formation of a Jordan-block structure in the spectral decomposition of the Liouvillian dynamics in the interior domain, as shown below. We notice that this degeneracy would be lifted if the normal form of the Hopf



bifurcation (26) was truncated after the quintic term instead of the cubic term, i.e., if  $c_4 \neq 0$ . In our cubic system, no further degeneracy occurs under the condition that

$$\frac{\omega - \mu\beta}{\omega} \neq \frac{n'}{n}, \quad \text{with } n, n' \in \mathbb{N}. \quad (95)$$

Now, we calculate the mean value (52) of an observable for the flow (47). After expanding both the observable and the initial density in Fourier series and after integrating over the angle  $\theta$ , we get

$$\begin{aligned} \langle A \rangle_t^{\text{in}} &= \sum_{n=-\infty}^{+\infty} e^{-in(\omega-\mu\beta)t} \int_0^{\sqrt{\mu}} dr \, r \left[ \frac{r^2}{\mu} + \left(1 - \frac{r^2}{\mu}\right) e^{-2\mu t} \right]^{in\beta/2} \rho_n(r) \\ &\quad \times A_n^* \left[ \frac{r}{\sqrt{\frac{r^2}{\mu} + \left(1 - \frac{r^2}{\mu}\right) e^{-2\mu t}}} \right]. \end{aligned} \quad (96)$$

In the limit  $t \rightarrow +\infty$ , this expression becomes

$$\langle A \rangle_t^{\text{in}} = \sum_{n=-\infty}^{+\infty} \langle A | \psi_{0n}^{\text{in}(c)} \rangle e^{s_{0n}^{(c)} t} \langle \tilde{\psi}_{0n}^{\text{in}(c)} | \rho \rangle + \mathcal{R}_0(t), \quad (97)$$

where the leading resonances are given by

$$s_{0n}^{(c)} = -i n (\omega - \mu\beta), \quad \text{with } n \in \mathbb{Z}, \quad (98)$$

their corresponding left and right eigenstates by

$$\begin{aligned} \langle A | \psi_{0n}^{\text{in}(c)} \rangle &= A_n^*(\sqrt{\mu}), \\ \langle \tilde{\psi}_{0n}^{\text{in}(c)} | \rho \rangle &= \int_0^{\sqrt{\mu}} dr \, r \left( \frac{r}{\sqrt{\mu}} \right)^{in\beta} \rho_n(r), \end{aligned} \quad (99)$$

and where the rest decays faster than the leading term

$$|\mathcal{R}_0(t)| < \mathcal{O}[\exp(-2\mu t) \exp(\varepsilon t)], \quad (100)$$

with  $\varepsilon > 0$ . We observe that the resonances (98) take the values given by Eq. (93) with  $l = 0$ , as expected. These resonances are associated with the limit cycle because the right eigenstates  $\psi_{0n}^{\text{in}(c)}$  have the limit cycle  $r = \sqrt{\mu}$  for support.

In order to obtain further resonances, we need to perform the asymptotic expansion of the rest in Eq. (97). We consider separately the contribution for zero Fourier index  $n = 0$ , and the other contributions for  $n \neq 0$ :

$$\mathcal{R}_0(t) = \mathcal{R}_{0,0}(t) + \sum_{n \neq 0} \mathcal{R}_{0,n}(t), \quad (101)$$

with

$$\begin{aligned} \mathcal{R}_{0,n}(t) &= e^{-in(\omega-\mu\beta)t} \int_0^{\sqrt{\mu}} dr \, r \left( \frac{r}{\sqrt{\mu}} \right)^{in\beta} \rho_n(r) \\ &\quad \times \left[ (1 + \zeta)^{in\beta/2} A_n^* \left( \sqrt{\frac{\mu}{1 + \zeta}} \right) - A_n^*(\sqrt{\mu}) \right], \quad \text{for } n = 0, 1, 2, 3, \dots, \end{aligned} \quad (102)$$

where we have introduced here again the quantity (87).

On the one hand, the contributions  $\mathcal{R}_{0,n}(t)$  with  $n \neq 0$  can be treated as the leading terms. Eq. (88) can here also be used at  $\zeta = 0^+$  instead of  $\zeta = 0^-$  in order to obtain

$$(1 + \zeta)^{in\beta/2} A_n^* \left( \sqrt{\frac{\mu}{1 + \zeta}} \right) = A_n^*(\sqrt{\mu}) + \frac{1}{2} \left( \frac{\mu}{r^2} - 1 \right) e^{-2\mu t} \left[ in\beta A_n^*(\sqrt{\mu}) - \sqrt{\mu} A_n^{*'}(\sqrt{\mu}) \right] + \dots \quad (103)$$

Inserting in Eq. (102), we get

$$\mathcal{R}_{0,n}(t) = \langle A | \psi_{1n}^{\text{in}(c)} \rangle e^{s_{1n}^{(c)} t} \langle \tilde{\psi}_{1n}^{\text{in}(c)} | \rho \rangle + \mathcal{R}_{1,n}(t), \quad (104)$$

with the next-to-leading resonances

$$s_{1n}^{(c)} = -2\mu - i n (\omega - \mu\beta), \quad \text{for } n \neq 0, \quad (105)$$

their corresponding left and right eigenstates

$$\begin{aligned} \langle A | \psi_{1n}^{\text{in}(c)} \rangle &= \frac{in\beta}{2} A_n^*(\sqrt{\mu}) - \frac{\sqrt{\mu}}{2} A_n'^*(\sqrt{\mu}), \\ \langle \tilde{\psi}_{1n}^{\text{in}(c)} | \rho \rangle &= \int_0^{\sqrt{\mu}} dr \left( \frac{r}{\sqrt{\mu}} \right)^{in\beta} \frac{\mu - r^2}{r} \rho_n(r), \quad \text{for } n \neq 0, \end{aligned} \quad (106)$$

and the rest

$$|\mathcal{R}_{1,n}(t)| < \mathcal{O}[\exp(-3\mu t) \exp(\varepsilon t)]. \quad (107)$$

According to the analyticity condition (60), we have that  $\rho_n(r) \sim r^{|n|}$  near the origin so that the integral of  $\langle \tilde{\psi}_{1n}^{\text{in}(c)} | \rho \rangle$  in Eq. (106) converges at  $r = 0$  under the condition  $n \neq 0$ . Therefore, the condition  $n \neq 0$  is consistently satisfied. The resonances (105) have the values expected from Eq. (93) with  $l = 1$ . They are also associated with the limit cycle because the right eigenstates have the limit cycle  $r = \sqrt{\mu}$  for support.

On the other hand, the contribution  $\mathcal{R}_{0,0}(t)$  corresponding to the case  $n = 0$  requires a separate treatment because it contains the asymptotic behavior caused by the degeneracy between the resonance of the limit cycle and another from the unstable focus both decaying as  $\exp(-2\mu t)$ . Since the unstable focus has an opposite stability with respect to the limit cycle, we need to perform a change of variables from the initial condition  $(r, \theta)$  to the current point at time  $t$  which is given by  $(r', \theta') = \Phi^t(r, \theta)$ . Thanks to the inverse mapping (49) and its Jacobian (50), we obtain

$$\mathcal{R}_{0,0}(t) = \int_0^{\sqrt{\mu}} dr' \frac{r' e^{-2\mu t}}{[1 + r'^2(e^{-2\mu t} - 1)/\mu]^2} \rho_0 \left[ \frac{r' e^{-\mu t}}{\sqrt{1 + r'^2(e^{-2\mu t} - 1)/\mu}} \right] [A_0^*(r') - A_0^*(\sqrt{\mu})]. \quad (108)$$

If we took the limit  $t \rightarrow \infty$  at this stage, we would encounter a problem because the integral of the leading term of the asymptotic expansion diverges at  $r' = \sqrt{\mu}$ . In order to cure this divergence, we separate the bracket in Eq. (108) as

$$A_0^*(r') - A_0^*(\sqrt{\mu}) = A_0^*(r') - A_0^*(\sqrt{\mu}) - A_0'^*(\sqrt{\mu}) \frac{r'^2 - \mu}{2\sqrt{\mu}} + A_0'^*(\sqrt{\mu}) \frac{r'^2 - \mu}{2\sqrt{\mu}}. \quad (109)$$

The last term of this equation is integrated by going back to the original variables  $(r, \theta)$ . At  $r = 0$ , another divergence appears which is treated with a similar method as in Eq. (109) but applied to the density  $\rho_0(r)$ . We obtain

$$\begin{aligned} \mathcal{R}_{0,0}(t) &= e^{-2\mu t} \int_0^{\sqrt{\mu}} dr' \frac{r'}{[1 + r'^2(e^{-2\mu t} - 1)/\mu]^2} \rho_0 \left[ \frac{r' e^{-\mu t}}{\sqrt{1 + r'^2(e^{-2\mu t} - 1)/\mu}} \right] \\ &\quad \times \left[ A_0^*(r') - A_0^*(\sqrt{\mu}) - A_0'^*(\sqrt{\mu}) \frac{r'^2 - \mu}{2\sqrt{\mu}} \right] \\ &- e^{-2\mu t} \frac{\sqrt{\mu}}{2} A_0'^*(\sqrt{\mu}) \int_0^{\sqrt{\mu}} dr r \frac{\mu - r^2}{r^2 + (\mu - r^2)e^{-2\mu t}} \left[ \rho_0(r) - \frac{\mu}{\mu - r^2} \rho_0(0) \right] \\ &- e^{-2\mu t} \frac{\mu^{3/2}}{2} A_0'^*(\sqrt{\mu}) \rho_0(0) \underbrace{\int_0^{\sqrt{\mu}} dr \frac{r}{r^2 + (\mu - r^2)e^{-2\mu t}}}_{=I}. \end{aligned} \quad (110)$$

The integral  $I$  in this equation can be carried out to get

$$I = \frac{\mu t}{1 - e^{-2\mu t}}. \quad (111)$$

The power law which appears is the evidence of the formation of a Jordan-block structure due to the degeneracy between the resonances corresponding to the invariant sets at  $r = 0$  and  $r = \sqrt{\mu}$ . We can now consider the asymptotic expansion of Eq. (110) for  $t \rightarrow \infty$ , and we get

$$\mathcal{R}_{0,0}(t) = e^{s_{10}^{(c)}t} \left[ \langle A|\psi_{10}^{(f)}\rangle \langle \tilde{\psi}_{10}^{(f)}|\rho\rangle + \langle A|\psi_{10}^{\text{in}(c)}\rangle \langle \tilde{\psi}_{10}^{\text{in}(c)}|\rho\rangle + t \langle A|\psi_{10}^{\text{in}(c)}\rangle \langle \tilde{\psi}_{10}^{(f)}|\rho\rangle \right] + \mathcal{O}(e^{-3\mu t}) , \quad (112)$$

with the next-to-leading resonance given by Eq. (93) with  $l = 1$  and  $n = 0$ ,

$$s_{10}^{(c)} = -2\mu , \quad (113)$$

and the corresponding Jordan block given by the root states

$$\begin{aligned} \langle A|\psi_{10}^{\text{in}(c)}\rangle &= -\frac{\sqrt{\mu}}{2} A_0^*(\sqrt{\mu}) , \\ \langle \tilde{\psi}_{10}^{\text{in}(c)}|\rho\rangle &= \int_0^{\sqrt{\mu}} dr \frac{\mu - r^2}{r} \left[ \rho_0(r) - \frac{\mu}{\mu - r^2} \rho_0(0) \right] , \end{aligned} \quad (114)$$

$$\begin{aligned} \langle A|\psi_{10}^{(f)}\rangle &= \int_0^{\sqrt{\mu}} dr' \frac{r'}{(\mu - r'^2)^2} \left[ A_0^*(r') - A_0^*(\sqrt{\mu}) - A_0^*(\sqrt{\mu}) \frac{r'^2 - \mu}{2\sqrt{\mu}} \right] , \\ \langle \tilde{\psi}_{10}^{(f)}|\rho\rangle &= \mu^2 \rho_0(0) . \end{aligned} \quad (115)$$

By comparing with Eq. (8), we infer that  $\psi_{10}^{(f)}$  is a right root state, while  $\tilde{\psi}_{10}^{\text{in}(c)}$  is a left root state of the Liouvillian operator. We observe that the right eigenstate  $\psi_{10}^{\text{in}(c)}$  has the limit cycle for support, while the left eigenstate  $\tilde{\psi}_{10}^{(f)}$  has the unstable focus for support. The integral of  $\langle \tilde{\psi}_{10}^{\text{in}(c)}|\rho\rangle$  converges at  $r = 0$  because the bracket vanishes as  $r$  at the origin. Moreover, the integral of  $\langle A|\psi_{10}^{(f)}\rangle$  converges at  $r = \sqrt{\mu}$  because the bracket vanishes as  $(r' - \sqrt{\mu})^2$  near the limit cycle.

In order to reveal the resonances associated with the unstable focus, we need to obtain the next-next-to-leading terms in our asymptotic expansion. For this purpose, we consider the rest  $\mathcal{R}_{1,n}(t)$  in Eq. (104), which we obtain by using the Taylor expansion (103):

$$\begin{aligned} \mathcal{R}_{1,n}(t) &= e^{-in(\omega - \mu\beta)t} \int_0^{\sqrt{\mu}} dr r \left( \frac{r}{\sqrt{\mu}} \right)^{in\beta} \rho_n(r) \\ &\times \left\{ (1 + \zeta)^{in\beta/2} A_n^* \left( \sqrt{\frac{\mu}{1 + \zeta}} \right) - A_n^*(\sqrt{\mu}) - \frac{\zeta}{2} \left[ in\beta A_n^*(\sqrt{\mu}) - \sqrt{\mu} A_n^*(\sqrt{\mu}) \right] \right\} , \end{aligned} \quad (116)$$

with  $n \neq 0$ . Since we expect a contribution from the unstable focus, we carry out a change to the variables  $(r', \theta')$  of the trajectory at the current time  $t$  by using the inverse flow (49) and the Jacobian (50). In these new variables, Eq. (87) becomes  $\zeta = (\mu/r'^2) - 1$ . An asymptotic expansion leads to the result

$$\mathcal{R}_{1,n}(t) = \langle A|\psi_{1n}^{(f)}\rangle e^{s_{1n}^{(f)}t} \langle \tilde{\psi}_{1n}^{(f)}|\rho\rangle + \mathcal{R}_{2,n}(t) , \quad (117)$$

where the next-next-to-leading eigenvalues is given by

$$s_{1n}^{(f)} = -3\mu - in\omega , \quad \text{with } n = \pm 1 , \quad (118)$$

the corresponding eigenstates by

$$\begin{aligned} \langle A|\psi_{1n}^{(f)}\rangle &= \int_0^{\sqrt{\mu}} dr' \frac{r'^{2+in\beta}}{(\mu - r'^2)^{\frac{5}{2} + i\frac{n\beta}{2}}} \\ &\times \left\{ \left( \frac{\mu}{r'^2} \right)^{in\beta/2} A_n^*(r') - A_n^*(\sqrt{\mu}) - \frac{1}{2} \left( \frac{\mu}{r'^2} - 1 \right) \left[ in\beta A_n^*(\sqrt{\mu}) - \sqrt{\mu} A_n^*(\sqrt{\mu}) \right] \right\} , \\ \langle \tilde{\psi}_{1n}^{(f)}|\rho\rangle &= \mu^{5/2} \rho_n'(0) , \end{aligned} \quad (119)$$

with  $n = \pm 1$ , and the rest satisfies

$$|\mathcal{R}_{2,n}(t)| < \mathcal{O}[\exp(-4\mu t)\exp(\varepsilon t)] . \quad (120)$$

We notice that  $\rho_n'(0) = 0$  for  $|n| \geq 2$ , so that the term (117) is non vanishing only for  $n = \pm 1$ . We remark that the convergence of the integral of  $\langle A|\psi_{1n}^{(f)}\rangle$  in Eq. (119) is guaranteed by the fact that the expression inside the brace is essentially the quadratic term of the Taylor expansion of  $(1 + \zeta)^{in\beta/2} A_n^* \left( \sqrt{\frac{\mu}{1+\zeta}} \right)$  which vanishes as  $(r' - \sqrt{\mu})^2$  near the limit cycle, whereupon, the integral converges.

Furthermore, we remark that, in the rest  $\mathcal{R}_{0,0}(t)$ , there exists another term of order  $e^{-3\mu t}$  which can be derived in a similar way, but it vanishes since it is proportional to  $\rho_0'(0) = 0$  [cf. Eq. (60)].

For the interior domain, the asymptotic expansion at long times of the average is therefore given by Eq. (97) where the rest  $\mathcal{R}_0(t)$  splits as shown in Eq. (101) into the term  $\mathcal{R}_{0,0}(t)$  given by Eq. (112) and further terms  $\mathcal{R}_{0,n}(t)$  given by Eq. (104). Moreover, the rest  $\mathcal{R}_{1,n}(t)$  of Eq. (104) is given by Eq. (117). These terms consistently give all the contributions which decay slower than  $\exp(-4\mu t)$ .

### 3. The full spectral decomposition

In order to obtain the spectral decomposition in both the interior and the exterior domains, the decompositions (89) and (97) [together with all the aforementioned terms given by Eqs. (101), (104), (112), & (117)] must be added according to Eq. (85). We note that the right eigenstates related to the limit cycle of the exterior and interior domains are the same:

$$\psi_{ln}^{\text{in}(c)} = \psi_{ln}^{\text{ex}(c)} \equiv \psi_{ln}^{(c)} , \quad l = 0, 1; \quad n = 0, \pm 1, \pm 2, \dots , \quad (121)$$

as shown by comparing Eq. (91) with Eqs. (99), (106), and (114). Hence, we finally obtain

$$\begin{aligned} \langle A \rangle_t &= \sum_{n=-\infty}^{+\infty} \langle A|\psi_{0n}^{(c)}\rangle e^{s_{0n}^{(c)}t} \langle \tilde{\psi}_{0n}^{(c)}|\rho \rangle \\ &+ \sum_{\substack{n=-\infty \\ n \neq 0}}^{+\infty} \langle A|\psi_{1n}^{(c)}\rangle e^{s_{1n}^{(c)}t} \langle \tilde{\psi}_{1n}^{(c)}|\rho \rangle \\ &+ \sum_{n=\pm 1} \langle A|\psi_{1n}^{(f)}\rangle e^{s_{1n}^{(f)}t} \langle \tilde{\psi}_{1n}^{(f)}|\rho \rangle \\ &+ \left( \langle A|\psi_{10}^{(c)}\rangle \quad \langle A|\psi_{10}^{(f)}\rangle \right) e^{s_{10}^{(c)}t} \begin{pmatrix} 1 & t \\ 0 & 1 \end{pmatrix} \begin{pmatrix} \langle \tilde{\psi}_{10}^{(c)}|\rho \rangle \\ \langle \tilde{\psi}_{10}^{(f)}|\rho \rangle \end{pmatrix} \\ &+ \mathcal{R}_2(t) , \end{aligned} \quad (122)$$

with the eigenvalues given by Eqs. (93) and (94), and with a rest decaying as

$$|\mathcal{R}_2(t)| < \mathcal{O}[\exp(-4\mu t)\exp(\varepsilon t)] . \quad (123)$$

The root states associated with the limit cycle are given by

$$\langle A|\psi_{0n}^{(c)}\rangle = A_n^*(\sqrt{\mu}) , \quad (124)$$

$$\langle A|\psi_{1n}^{(c)}\rangle = \frac{i\beta n}{2} A_n^*(\sqrt{\mu}) - \frac{\sqrt{\mu}}{2} A_n^{*l}(\sqrt{\mu}) , \quad (125)$$

$$\langle \tilde{\psi}_{0n}^{(c)}|\rho \rangle = \int_0^\infty dr r \left( \frac{r}{\sqrt{\mu}} \right)^{in\beta} \rho_n(r) , \quad (126)$$

$$\langle \tilde{\psi}_{1n}^{(c)}|\rho \rangle = \int_0^\infty dr \left( \frac{r}{\sqrt{\mu}} \right)^{in\beta} \frac{\mu - r^2}{r} \rho_n(r) , \quad (n \neq 0) , \quad (127)$$

$$\langle \tilde{\psi}_{10}^{(c)}|\rho \rangle = \int_0^\infty dr \frac{\mu - r^2}{r} \left[ \rho_0(r) - \frac{\mu}{\mu - r^2} \theta(\sqrt{\mu} - r) \rho_0(0) \right] , \quad (128)$$

where  $\theta(\sqrt{\mu} - r)$  is the Heaviside function. Besides, the root states associated with the unstable focus are given by Eqs. (115) and (119).

The first term in Eq. (122) corresponds to the oscillation on the limit cycle. The other terms decay exponentially to zero and correspond to the relaxation of the probability density which is attracted by the limit cycle and repelled by the unstable focus.

The asymptotic expansion is here consistently truncated at terms of the order of (123). The rest of the asymptotic expansion can be obtained by recurrence. These following terms will correspond to the different resonances depicted in Fig. 5. As  $\text{Re } s \rightarrow -\infty$ , the resonance spectrum presents a structure of periodicity  $-2\mu$ , as observed in Fig. 5. Within each period, we find an infinite number of resonances associated with the limit cycle that produce terms similar to those in the second line of Eq. (122), and a growing finite number of resonances associated with the unstable focus that produce terms similar to those of the third line. At zero frequency, the double degeneracies yield second-order Jordan blocks similar to the one in the fourth line.

## V. CONCLUSIONS

In this paper, we have constructed the spectral decomposition of the Liouvillian dynamics of nonlinear vector fields undergoing a Hopf bifurcation, which is the major bifurcation giving birth to oscillatory behavior in far-from-equilibrium dissipative systems. The Liouvillian dynamics rules the time evolution of statistical ensembles of deterministic trajectories issued from random initial conditions.

Our present work reveals that the oscillations occurring near a Hopf bifurcation manifest themselves in the Liouvillian spectrum by the existence of complex resonances with real frequencies. We have shown that the Liouvillian spectrum is discrete before and after the Hopf bifurcation while the discrete spectrum collapses into a continuous spectrum at criticality.

We have shown in Sec. IV D that the power-law relaxation at the transition, a phenomenon also referred to as critical slowing down, can be explained by the continuous Liouvillian spectrum at criticality. In the light of the previous work on the Liouvillian spectrum near a pitchfork bifurcation [8], a continuous spectrum appears to be a general feature of far-from-equilibrium systems undergoing a bifurcation. In the pitchfork bifurcation, the continuous spectrum is purely real because of the absence of oscillation near this bifurcation [8]. However, in the Hopf bifurcation, the continuous spectrum extends to complex eigenvalues because of the emerging oscillations, as shown in Sec. IV D.

Away from the bifurcation, the Liouvillian spectrum is discrete and composed of a countable set of resonances which are the analogues of the Pollicott-Ruelle resonances in the present system.

Before the Hopf bifurcation, all these complex resonances have a non-vanishing relaxation rate because the oscillations are damped in the subcritical regime. All the subcritical resonances are associated with the stable focus which attracts the trajectories and, therefore, the probability density. Consequently, the right eigenstates of the spectral decomposition have the stable focus for support in the subcritical regime, as shown in Sec. IV C.

After the Hopf bifurcation, there exist purely imaginary resonances with a real frequency and a vanishing relaxation rate. These resonances describe the time evolution of statistical ensembles of trajectories on the attracting periodic orbit. The resonance at zero frequency and relaxation rate corresponds to the eigenstate with a stationary distribution along the limit cycle, while the other resonances with non-zero frequencies describe the oscillations of the mean values or time-correlation functions and, especially, the harmonics of the periodic but nonlinear asymptotic time evolution. The existence of all these purely imaginary resonances shows that the system is non-mixing. The resonances with a non-vanishing relaxation rate describe the evolution of the probability density which is repelled by the unstable focus and attracted by the limit cycle.

On the one hand, the periodic orbit contributes to the Liouvillian spectrum by an array of resonances filling a half-lattice, as seen in Figs. 3 or 5. On the other hand, the unstable focus contributes to the spectrum by a pyramidal array of resonances, also seen in Figs. 3 or 5. Contrary to the subcritical pyramidal array depicted in Fig. 2, the supercritical one is not centered on the origin but on a resonance with a non-vanishing relaxation rate and a zero frequency. This feature has its direct origin in the fact that the focus is unstable after criticality, although it is stable before criticality.

In the cubic vector field which we have studied in detail in Sec. IV, the zero-frequency resonances of the unstable focus turn out to be degenerate with some zero-frequency resonances of the limit cycle, as it is the case in Fig. 5 (but not in Fig. 3). As the consequence of these degeneracies, a Jordan-block structure appears in the spectral decomposition, leading to special asymptotic time evolutions in which the exponential relaxation is multiplied by a positive power of the time, such as  $t \times \exp(-2\mu t)$ .

For a generic vector field with terms of quintic or higher degrees, these degeneracies and the related Jordan blocks would not occur because no degeneracy happens generically between the resonances of the limit cycle and those of the unstable focus, as seen in Fig. 3.

In conclusion, the present work shows how the periodic-orbit theory of classical dissipative systems must be extended to include the effect of stationary states coexisting with periodic orbits. These stationary states contribute to the trace formula of the Frobenius-Perron operator by extra terms involving the linear stability eigenvalues of the stationary states, as shown in Sec. II C. These extra terms are responsible for the existence of the further resonances associated with the stationary states. Moreover, the methods developed in the present paper allows us to obtain not only the full spectrum of Liouvillian resonances but also the associated eigenstates (and other root states in the presence of Jordan-block structures). These time-asymptotic methods are therefore particularly powerful and promising for the study of time-dependent phenomena in nonlinear dynamical systems.

In a future publication, we shall present a systematic method to construct the full spectral decomposition and we shall give the proof of its convergence.

**Acknowledgments.** We thank Professor G. Nicolis for support and encouragement in this research. P. G. is financially supported by the National Fund for Scientific Research (F. N. R. S. Belgium). This research is supported, in part, by the Interuniversity Attraction Pole program of the Belgian Federal Office of Scientific, Technical and Cultural Affairs, by the National Fund for Scientific Research (F. N. R. S. Belgium), by Grants-in-Aid (B) and (C) for Scientific Research from the Japan Society for the Promotion of Science (JSPS). This work is also a part of the project of the Institute for Fundamental Chemistry, supported by JSPS - Research for the Future Program (JSPS-RFTF96P00206).

- 
- [1] G. Nicolis, *Introduction to Nonlinear Science* (Cambridge University Press, Cambridge, 1995).
  - [2] R. Artuso, E. Aurell, and P. Cvitanović, *Nonlinearity* **3**, 325, 361 (1990).
  - [3] P. Cvitanović and B. Eckhardt, *J. Phys. A: Math. Gen.* **24**, L237 (1991).
  - [4] P. Gaspard, *Chaos, Scattering, and Statistical Mechanics* (Cambridge University Press, Cambridge, 1998).
  - [5] P. Gaspard, *J. Phys. A: Math. Gen.* **25**, L483 (1992); P. Gaspard, *Phys. Lett. A* **168**, 13 (1992).
  - [6] S. Tasaki, I. Antoniou, and Z. Suchanecki, *Phys. Lett. A* **179**, 97 (1993); S. Tasaki, I. Antoniou, and Z. Suchanecki, *Chaos, Solitons, and Fractals* **4**, 227 (1994).
  - [7] P. Gaspard and D. Alonso Ramirez, *Phys. Rev. A* **45**, 8383 (1992).
  - [8] P. Gaspard, G. Nicolis, A. Provata, and S. Tasaki, *Phys. Rev. E* **51** (1995) 74.
  - [9] W. Lu, L. Viola, K. Pance, M. Rose, and S. Sridhar, *Phys. Rev. E* **61**, 3652 (2000).
  - [10] K. Pance, W. Lu, and S. Sridhar, *Phys. Rev. Lett.* **85**, 2737 (2000).
  - [11] M. Pollicott, *Invent. Math.* **81**, 413 (1985); **85**, 147 (1986).
  - [12] D. Ruelle, *Phys. Rev. Lett.* **56**, 405 (1986); *J. Stat. Phys.* **44**, 281 (1986); *J. Diff. Geom.* **25**, 117 (1987); *Commun. Math. Phys.* **125**, 239-262 (1989).
  - [13] E. Hopf, *Berichten der Mathematisch-Physischen Klasse der Sächsischen Akademie der Wissenschaften zu Leipzig*. XCIV. Band Sitzung vom 19. Januar 1942. An English translation is given in [14].
  - [14] J. E. Marsden and M. McCracken, *The Hopf Bifurcation and Its Applications* (Springer, New York, 1976).
  - [15] V. I. Arnold, *Geometrical Methods in the Theory of Ordinary Differential Equations* (Springer, New York, 1983).
  - [16] J. Guckenheimer and P. Holmes, *Nonlinear Oscillations, Dynamical Systems, and Bifurcations of Vector Fields* (Springer, New York, 1983).
  - [17] G. Nicolis and M. Malek Mansour, *Prog. Theor. Phys. Suppl.* **64**, 249 (1978).
  - [18] N. G. van Kampen, *Stochastic Processes in Physics and Chemistry* (North-Holland, Amsterdam, 1981).
  - [19] F. Baras, M. Malek Mansour, and C. Van Den Broeck, *J. Stat. Phys.* **28**, 577 (1982).
  - [20] F. Baras, J. E. Pearson, and M. Malek Mansour, *J. Chem. Phys.* **93**, 5747 (1990).
  - [21] M. Mareschal and A. De Wit, *J. Chem. Phys.* **96**, 2000 (1992).
  - [22] I. Prigogine, *Nonequilibrium Statistical Mechanics* (Wiley, New York, 1962).
  - [23] I. C. Gohberg and M. G. Klein, *Introduction à la théorie des opérateurs linéaires non auto-adjoint dans un espace hilbertien* (Dunod, Paris, 1971).
  - [24] N. Dunford and J. T. Schwartz, *Linear operators*, Vols. I-III (Interscience-Wiley, New York, 1958, 1963, 1971).
  - [25] I. Gel'fand and G. Shilov, *Generalized Functions*, Vol. 2 (Academic Press, New York, 1968).
  - [26] D. V. Widder, *The Laplace transform* (Princeton University Press, Princeton NJ, 1941).